

Synthesis of tri-aryl ketone amine isomers and their cure with epoxy resins

Reyes, Larry Q.; Dao, Buu; Vogel, Wouter; Bijleveld, Johan; Tucker, Sam; Christensen, Steve; Wiggins, Jeffrey; Dingemans, Theo; Varley, Russell J.

DOI

[10.1002/pat.4818](https://doi.org/10.1002/pat.4818)

Publication date

2019

Document Version

Accepted author manuscript

Published in

Polymers for Advanced Technologies

Citation (APA)

Reyes, L. Q., Dao, B., Vogel, W., Bijleveld, J., Tucker, S., Christensen, S., Wiggins, J., Dingemans, T., & Varley, R. J. (2019). Synthesis of tri-aryl ketone amine isomers and their cure with epoxy resins. *Polymers for Advanced Technologies*, 31(4), 827-837. <https://doi.org/10.1002/pat.4818>

Important note

To cite this publication, please use the final published version (if applicable).
Please check the document version above.

Copyright

Other than for strictly personal use, it is not permitted to download, forward or distribute the text or part of it, without the consent of the author(s) and/or copyright holder(s), unless the work is under an open content license such as Creative Commons.

Takedown policy

Please contact us and provide details if you believe this document breaches copyrights.
We will remove access to the work immediately and investigate your claim.

Synthesis of tri-aryl ketone amine isomers and their cure with epoxy resins

Abstract

Isomeric tri-aryl ketone amines, 1,3-bis(3-aminobenzoyl)benzene (133 BABB), 1,3-bis(4-aminobenzoyl)benzene (134 BABB), and 1,4-bis(4-aminobenzoyl)benzene (144 BABB) are synthesized and cured with diglycidyl ether of bisphenol A and diglycidyl ether of bisphenol F in this work. Differential scanning calorimetry and near-infrared spectroscopy reveal higher rate constants and enhanced secondary amine conversion with increasing para substitution attributed to resonance effects and the electron withdrawing nature of the carbonyl linkages. Glass transition temperatures increase from 133 BABB to 134 BABB, but decrease modestly for the 144 BABB hardener. With increasing para substitution, the flexural modulus and strength both decrease while the strain to failure increases but all BABB amines displaying higher mechanical properties than the corresponding 4,4-diaminodiphenyl sulfone (44 DDS) networks. The thermal stability of the BABB networks is found to be modestly lower than 44 DDS, but char yields are significantly higher. Changes in thermal and mechanical properties are described in terms of molecular structure and equilibrium packing density.

1 INTRODUCTION

Epoxy resins continue to be the polymer matrix most widely used in structural composite materials because of their superior mechanical and thermal properties and comparative ease of processability.^{1, 2} Demanding design specifications and performance requirements, however, continue to place increased demands upon the matrix resin for next generation composite materials. A lack of toughness or distortional behavior of the matrix in particular, is driving much of the current research into more ductile and impact resistant network polymers.³⁻⁵ Despite being primarily controlled by crosslink density or the chemical structure of the network, additive approaches to improving toughness are common, including ductile and rigid inclusions,⁶⁻⁸ interlayers,^{9, 10} and nanoadditives¹¹⁻¹³ to name a few. The primary goal of all these strategies, however, remains the enhancement of toughness or distortional behavior, without compromising other desirable properties such as modulus, strength, or processability.^{5, 12, 14}

More recent studies have focused upon improving the intrinsic toughness or distortional response to deformation of the epoxy amine network using flexible comonomers^{15, 16} or controlling local mobility of the network rather than using additives.¹⁷⁻¹⁹ Ramsdale-Capper and Foreman¹⁸ explored the impact of local molecular mobility as determined by the γ and β relaxations of the network on macroscopic properties, simply by altering the aromatic substitution from meta to para on the epoxy or amine. Fracture toughness was observed to be higher for a meta substituted amine, which was attributed to an internal

anti-plasticization effect and a lack of phenylene rotations. This work supported other studies which suggested that the restriction of phenylene rotations for meta substituted systems reduced free volume to create a kind of molecular reinforcement that increased modulus.^{19, 20} Varley et al²⁰ also reported similar results for isomeric tri-aryl ether amine resin systems cured with an epoxy resin where they differed only in their aromatic substitution patterns. Increases in strength and stiffness for increasingly meta substituted amines were observed, while conversely yield strain and glass transition temperatures both increased with increasing para substitution. The design of novel multiaromatic amines was taken a step further by Misasi²¹ who synthesized four, five, and six membered aromatic ringed aryl ether ketone amine curatives for epoxy resins. In this work, the aryl ether linkages were reported to be a source of local molecular mobility and hence an energy dissipation mechanism while the aryl ketone linkages increased stiffness. This was attributed to the reduced flexibility of the ketone linkage and the supplementary reinforcement arising from a higher degree of meta substitution. These studies represent an attempt to understand the molecular origin of the macroscale properties of highly aromatic crosslinked epoxy amine networks and provide new insights and new approaches to overcoming brittle behavior in epoxy networks.

The investigation here continues this research trajectory using a novel series of multi-aromatic amines as curatives for commercial epoxy resins to explore improvements in thermal and mechanical properties. Three tri-aryl ketone amine isomers, varying only in their aromatic substitution were synthesized and cured with commercially available epoxy resins, diglycidyl ether of bisphenol F (BisF), and diglycidyl ether of bisphenol A (BisA). Their mechanical and thermal properties were evaluated as was the impact upon resin kinetics, while the network structure of the cured network was investigated using near-infrared (NIR) spectroscopy. The epoxy resins were also cured with 4,4-diaminodiphenyl sulfone (44 DDS) systems to serve as a commercial benchmark to the aryl ketone amine networks.

2 EXPERIMENTAL

2.1 Materials

Diglycidyl ether of BisF, EPON 862 (EEW 165-173 g/eq.) and diglycidyl ether of BisA, DER331 (EEW 182-192 g/eq) were obtained from Momentive Chemicals (Malaysia) and the Dow Chemical Company, respectively. Both epoxy resins were degassed in a vacuum oven and dried at 90°C for 12 hours prior to use. The 44 DDS (>98%) was purchased from TCI Chemicals (Japan) and used without further purification. The chemical structures of BisF, BisA, and 44 DDS are shown in Figure 1. All other chemicals and solvents involved with the synthesis of the aryl ketone amines were used as received from Sigma-Aldrich, TCI, or VWR.

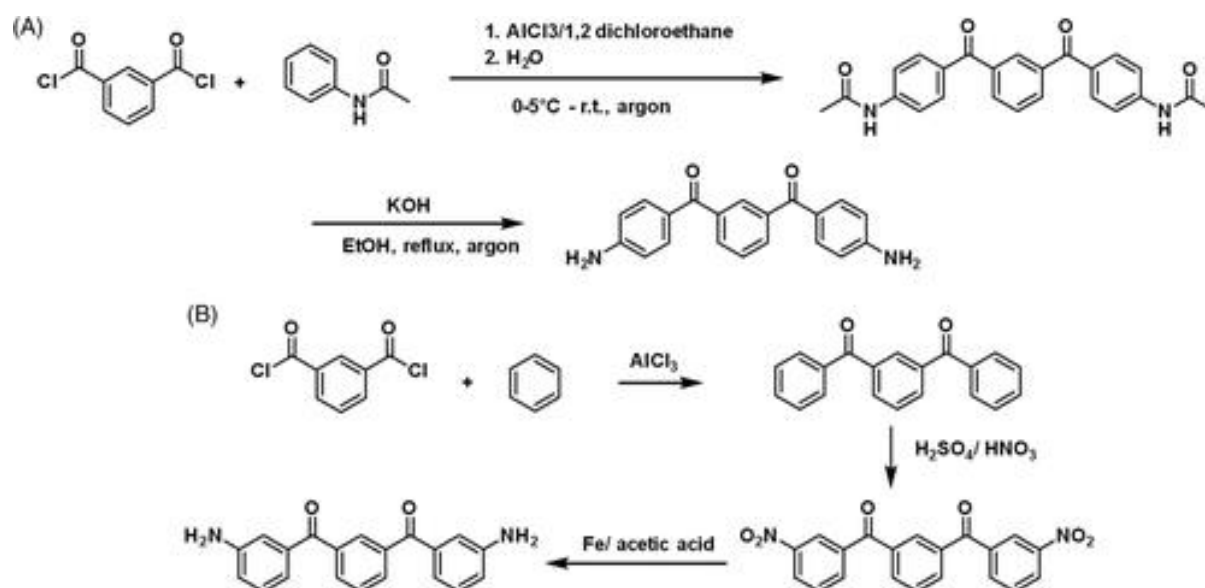


Figure 1

Open in figure viewerPowerPoint

Experimental protocols to synthesize (A) 134 BABB and (B) 133 BABB hardeners. Note that synthesis of 144 BABB is identical to 134 BABB except starting acyl chloride is para substituted

^1H and ^{13}C NMR spectra were recorded in CDCl_3 or $\text{DMSO}-d_6$ on an Agilent NMR system (400 MHz for ^1H , 100 MHz for ^{13}C) at 20°C to 25°C . ^1H NMR spectra are reported in parts per million using the residue solvent signal (2.50 for $\text{DMSO}-d_6$ and 7.26 for CDCl_3) as an internal standard. The data of ^1H NMR are reported as follows: chemical shift, multiplicity (s = singlet, d = doublet, t = triplet, m = multiplet), coupling constants (J , Hz), and integration. ^{13}C NMR spectra are reported in parts per million using solvent CDCl_3 ($\delta = 77.2$ ppm) or $\text{DMSO}-d_6$ ($\delta = 39.5$ ppm) as an internal standard. Mass spectra are measured in a Shimadzu GCMS QP2010S using a direct inlet with electron impact as the ionization method. Infrared spectra of the amine products were obtained using a PerkinElmer Spectrum 100 equipped with a Diamond ATR accessory. The infrared absorptions are given in cm^{-1} . Thermal stability and melting points are measured using a PerkinElmer TGA4000 thermogravimetric analyzer and a PerkinElmer DSC8000 differential scanning calorimetry (DSC) at a rate of $10^\circ\text{C min}^{-1}$. Melting temperatures are given as peak values of the endothermic peak.

2.2 Synthesis of tri-aryl ketone amines

The tris-aryl ketone amine isomers, 1,3-bis(3-aminobenzoyl)benzene (133 BABB), 1,3-bis(4-aminobenzoyl)benzene (134 BABB), and 1,4-bis(4-aminobenzoyl)benzene (144 BABB) were synthesized using Friedel-Crafts acylation reactions according to the reaction sequences in Figure 2. In the case of 134 and 144 BABB, phenylacetamide was used which was subsequently hydrolyzed to produce para substituted amines on the outer aromatic rings. Synthesis of the 133 BABB used benzene that required nitration via meta directed

electrophilic substitution which could be subsequently reduced to an amine. All reactions were performed in an inert atmosphere.

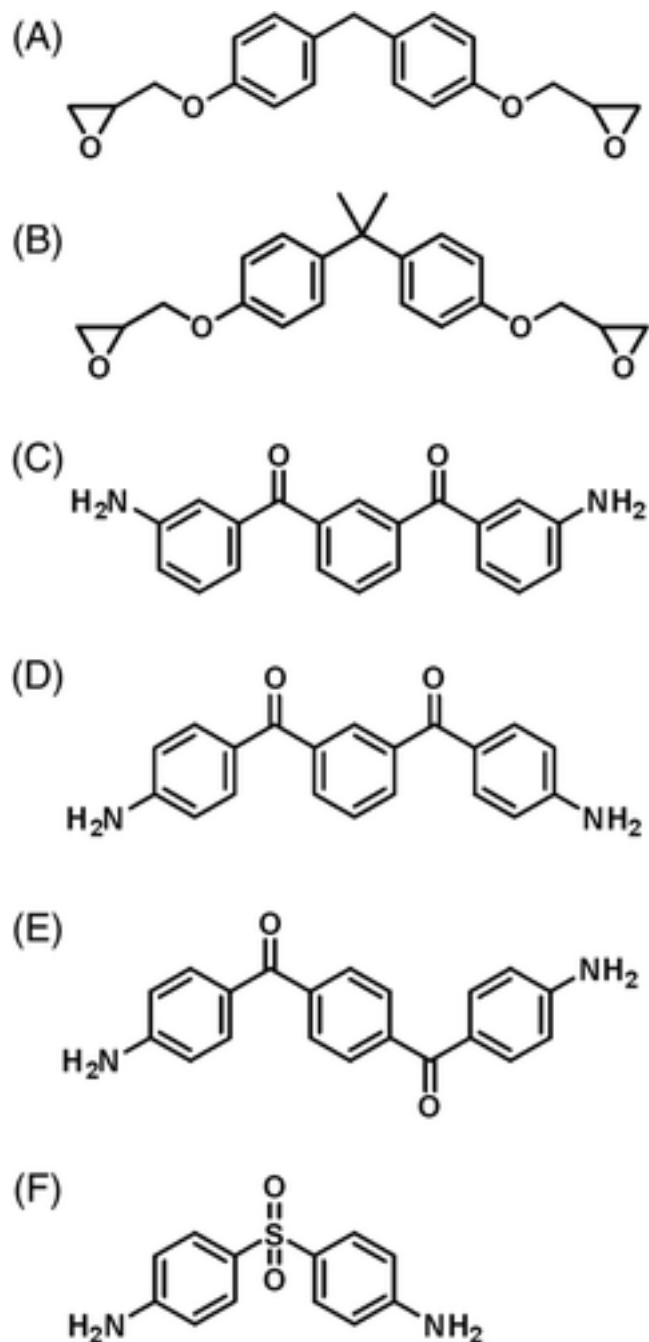


Figure 2

[Open in figure viewerPowerPoint](#)

Chemical structures of the (A) BisF and BisA epoxy resins, (B) 133 BABB, (C) 134 BABB, (D) 144 BABB, and (E) 44 DDS

2.2.1 Synthesis of 144 BABB

1,4 Bis(4-acetamidebenzoyl)benzene

To a vigorously stirred solution of 25.32 g 1,4-isophthaloyl dichloride (81 mmol) in 125 mL CH_2Cl_2 , 64.28 g of powdered AlCl_3 (0.48 mol) was added. This mixture was cooled with an ice bath, after which 21.8 g of acetanilide (0.158 mol) was slowly added. The reaction mixture was stirred overnight and poured into 2.5 L of ice water. The resulting suspension was allowed to reach room temperature and filtered. The solids were stirred twice with demineralized water (2 L) then collected and dried, yielding 34.01 g of a white powder.

$^1\text{H-NMR}$ (DMSO): 10.31 (s, 2H), 8.09 (t, 1H, $J = 7.6$ Hz), 7.78 (m, 11H), 2.11 (s, 6H). $^{13}\text{C-NMR}$: 193.8, 168.8, 143.6, 140.2, 139.4, 131.1, 130.5, 129.6, 129.0, 125.3, 118.0, 24.0.

1,4-Bis(4-aminobenzoyl)benzene

Here, 30.4 g of the dried solids were added to a solution of 22.0 g of KOH (0.39 mol) in 250 mL of ethanol and heated to reflux. After approximately 15 minutes, a bright yellow precipitate formed. The precipitate was collected and stirred with hot deionized water (1 L). Filtration yielded 18.45 g (58 mmol) of a bright yellow powder.

$^1\text{H-NMR}$ (DMSO): 7.66 (s, 4H), 7.55 (d, 4H, $J = 8.8$ Hz), 6.60 (d, 4H, $J = 8.8$ Hz), 6.21 (s, 4H). $^{13}\text{C-NMR}$: 193.2, 154.5, 141.5, 133.1, 128.9, 123.8, 113.0. MS: Calculated M^+ ($\text{C}_{20}\text{H}_{16}\text{N}_2\text{O}_2$): 316.12, Found: 316.00. IR: 3346, 1628, 1580, 1317, 1276, 1156, 926, 832, 747, 690. $T_d, 5\%$: 342°C, T_m : 285°C.

2.2.2 Synthesis of 134 BABB

1,3 Bis(4-acetamidebenzoyl)benzene

To a vigorously stirred solution of 61.6 mL 1,3-isophthaloyl dichloride (100.3 g, 0.32 mol) in 500 mL CH_2Cl_2 , 255.8 g of powdered AlCl_3 (1.92 mol) was added. This mixture was cooled with an ice bath, after which 86.44 g of acetanilide (0.63 mol) was slowly added. The reaction mixture was stirred overnight then poured into 8 L of ice water. The resulting suspension was allowed to reach room temperature and filtered. The solids were stirred with NaOH solution (0.5 M, 5 L), and twice with deionized water (4 L) then collected and dried to yield 127 g (0.31 mmol, 99%) of the title compound.

$^1\text{H-NMR}$ (DMSO): 10.33 (s, 2H), 7.95 (d, 2H, $J = 7.6$ Hz), 7.92 (s, 1H), 7.76 (m, 7H), 2.08 (s, 6H). $^{13}\text{C-NMR}$: 193.5, 168.8, 143.4, 137.3, 132.5, 131.0, 130.9, 129.7, 128.6, 117.9, 23.9.

1,3-Bis(4-aminobenzoyl)benzene

Then, 41.0 g (0.102 mol) of the dried solids were added to a solution of 28 g of KOH (0.49 mol) in 250 mL of ethanol and heated to reflux. After approximately 15 minutes, a bright yellow precipitate formed which was collected then stirred in hot deionized water (1 L). Filtration yielded 27.74 g (88 mmol) of the title compound as a gray powder.

$^1\text{H-NMR}$ (DMSO): 7.80 (d, 2H, $J = 6.4$ Hz), 7.74 (s, 1H), 7.64 (t, 1H, $J = 6.8$ Hz), 7.55 (d, 4H, $J = 6.8$ Hz), 6.61 (d, 4H), 6.21 (s, 4H). $^{13}\text{C-NMR}$: 193.1, 154.4, 139.2, 133.1, 131.7, 129.4, 128.8, 123.8, 113.0. MS: Calculated M^+ ($\text{C}_{20}\text{H}_{16}\text{N}_2\text{O}_2$):316.12, Found: 316.05. IR: 3337, 1644, 1624, 1585, 1544, 1443, 1312, 1158, 750. $T_{d, 5\%}$: 350°C, T_m : 242°C.

2.2.3 Synthesis of 133 BABB

1,3-Bis(benzoyl)benzene

To a solution of 32.84 g of 1,3-isophthaloyl dichloride (0.16 mol) in 310 mL of benzene, 42 g of AlCl_3 (0.31 mol) was added slowly. Some gas evolution was observed during the addition. The reaction mixture was stirred at room temperature overnight, after which it was poured out on 500 mL ice-cold water. The resulting suspension was stirred for 1 hour, after which the excess benzene was evaporated under reduced pressure. The solids were then filtered and washed once with a NaOH solution (10%, 400 mL), then twice with deionized water. After drying at 60°C in vacuum, the desired compound yielded 41.92 g (0.15 mol, 91%) as a white powder.

$^1\text{H-NMR}$ (CDCl_3): 8.18 (s, 1H), 8.02 (d, 2H, $J = 8.0$ Hz), 7.81 (d, 4H, $J = 7.2$ Hz), 7.61 (m, 3H), 7.49 (t, 4H, $J = 7.6$ Hz). $^{13}\text{C-NMR}$: 195.8, 137.8, 137.0, 133.4, 132.8, 131.2, 130.1, 128.5, 128.4.

1,3-Bis(3-nitrobenzoyl)benzene

To an ice-cooled solution of 20.05 g (70 mmol) of 1,3-bis(benzoyl)benzene in 80 mL of concentrated sulfuric acid, a mixture of 14 mL nitric acid (65%) (70 mmol) and 40 mL of concentrated sulfuric acid was added dropwise. After stirring for 30 minutes, the reaction mixture was poured into 1 L of ice then filtered and washed again with 600 mL of water. After filtration, the solid was dried and recrystallized from butanone (200 mL). This yielded 13.24 g (0.35 mmol, 50%) of the title compound as a white solid.

$^1\text{H-NMR}$ (DMSO): 8.64 (s, 2H), 8.46 (d, 2H, $J = 8.0$ Hz), 8.16 (d, 2H, $J = 7.2$ Hz), 8.09 (d, 2H, $J = 8.4$ Hz), 7.73 (double triplet, 3H, $J = 8.0$ Hz) $^{13}\text{C-NMR}$: 192.9, 148.2, 138.2, 136.9, 135.3, 134.2, 131.0, 130.0, 129.5, 127.2, 124.6.

1,3-Bis(3-aminobenzoyl)benzene

To a suspension of 12.19 g of 1,3-bis(3-nitrobenzoyl)benzene in 240 mL of ethanol, 240 mL of glacial acetic acid and 10 mL of water, 45 g of iron powder (~325 mesh) was added in one portion. This mixture was refluxed for 3 hours, after which it was filtered, and the filter cake was flushed with ethyl acetate. The liquids were neutralized and extracted with ethyl acetate. The organic layers were washed with water and brine solution. The solvent was evaporated under reduced pressure, yielding a golden-yellow powder.

¹H-NMR (DMSO): 7.99(d, 2H, *J* = 7.6 Hz), 7.94 (s, 1H), 7.73 (t, 1H, *J* = 7.6 Hz), 7.19 (t, 2H, *J* = 7.6 Hz), 6.97 (s, 2H), 6.87 (d, 2H, *J* = 7.6 Hz), 6.84 (d, 2H, *J* = 8.0 Hz), 5.43 (s, 4H). ¹³C-NMR: 196.0, 149.4, 137.9, 137.7, 133.4, 130.7, 129.5, 129.4, 118.7, 117.7, 114.9. MS: Calculated $M^+(C_{20}H_{16}N_2O_2)$:316.12, Found: 316.15. IR: 3356, 1650, 1579, 1452, 1314, 1219, 728. $T_{d, 5\%}$: 296°C.

2.3 Sample preparation

The BisF and BisA epoxy resins were cured with 133 BABB, 134 BABB, and 144 BABB and 44 DDS using a 1:1 epoxide to amino stoichiometric ratio. The amines were added to the epoxy resin and mixed and degassed using a rotary evaporator at a temperature of 110°C for 30 minutes or until completely dissolved and free of bubbles. The samples were placed in an oven already equilibrated at the set temperature of 177°C and after curing for 10 hours was allowed to cool down slowly to room temperature.

2.4 Characterization

2.4.1 Thermal analysis

A PerkinElmer SII Seiko Instruments Sapphire DSC was used to characterize the cure kinetics, reaction rates, and glass transition temperatures of the cured networks. For the dynamic experiment, the uncured resin was placed in the DSC oven at 50°C and heated to 300°C at a rate of 10°C/min. The network was then cooled to 50°C and ramped again to 300°C at 10°C/min. For the isothermal experiment, performed in duplicate, the uncured resin was cured in the DSC oven at 177°C for 10 hours then cooled to room temperature and also subjected to a similar dynamic rescan after cure. For the larger-scale samples taken from the resin cured in the oven in silicone molds, analysis was performed by heating approximately 10 mg of the cured resins from 50°C to 300°C at a rate of 10°C/min. At all times, DSC experiments were performed under a blanket of nitrogen.

Dynamic mechanical thermal analysis (DMTA) was performed using a PerkinElmer SEIKO DMA Diamond II Series. Samples of approximate dimensions 10 × 50 × 2.8 mm³ were placed in a dual cantilever fixture using a force amplitude of 20 μm and a frequency of 1 Hz. Samples were heated from 50°C to 250°C at a rate of 2°C/min while applying the stress and frequency in the bending mode. The glass transition temperatures, T_g , were determined from the peak in the tan δ spectra.

Thermal stability of the cured samples was investigated using a Mettler Toledo 821^eTGA/SDTA thermogravimetric analyzer (TGA). About 10 mg of the cured samples were placed in a ceramic crucible and heated from 50°C to 600°C at a rate of 10°C/min under a nitrogen gas environment. Samples were characterized-based upon the temperature at 10%

mass loss, $T_{10\%}$, the temperature at the maximum rate of degradation, T_{max} , and the char yield at 600°C.

2.4.2 NIR spectroscopy

NIR spectra were determined using a Nicolet 6700 Spectrometer FTIR in transmission mode. Samples of approximate dimensions, $20 \times 20 \times 3 \text{ mm}^3$ were placed in the beam and measurement was made in the range of 4000 to 7000 cm^{-1} by taking an average of 32 scans.

2.4.3 Flexural properties

The flexural properties were measured using an Instron 3880 Universal Testing Machine fitted with a 1 kN load cell configured in the three-point bending mode. The crosshead rate used was 1 mm/min and testing continued until the sample failed. The span to depth ratio was kept constant at 16:1 using the as-prepared samples. All results reported are an average of at least three replicates.

2.4.4 Computational methods

Force field calculations were employed to determine the equilibrium molecular geometry (MM2 Energy minimization, minimum of 10,000 iterations), amine-to-amine distance of the curing agent and end-to-end distance of the epoxy monomer using the PerkinElmer Chem3D program. All calculations assumed that the molecules existed in the ground state and in vacuum.

3 RESULTS AND DISCUSSION

3.1 Cure kinetics and network structure

Dynamic DSC thermograms of the uncured BisF resins in Figure **3** each exhibit large peaks typically associated with the exothermic reaction of epoxy amine resins during cure. Systematic differences were clearly observed between the different BABB hardeners in regard to the breadth of the exothermic peak, T_p , the temperature at the max heat output, and T_{onset} , the temperature where the exothermic reaction first starts to occur. The T_p and T_{onset} both increase consistently with increasing para substitution of BABB for BisF, while Table **1** shows that similar trends also exist for the BisA epoxy resins. While not directly determining the rate of reaction, these parameters do reflect the ease of reaction such that a higher T_p and T_{onset} can still be regarded as an indicator of a slower cure reaction. Therefore, for both BisF and BisA, this experiment suggests that 144 BABB amine is the slowest curative, followed by 134 BABB and then 133 BABB, being the fastest. The similarity between the T_p and T_{onset} of the 44 DDS and 134 BABB systems, also implies that 134 BABB about the same or a little faster than the 44 DDS. This is important in light of the fact that 44 DDS is the most important aromatic amine curative used commercially for

structural composite applications. Another noticeable difference between the thermograms for both the BisF and BisA epoxy resins is that the width of the exothermic curing peaks becomes narrower with increasing para substitution from 133 BABB to 144 BABB. While the reasons for this are not fully understood, it may reflect the formation of a less homogenous network arising from the presence of cis and trans conformers¹⁸ in the 133 BABB and 134 BABB amines, not available to the 144 BABB.

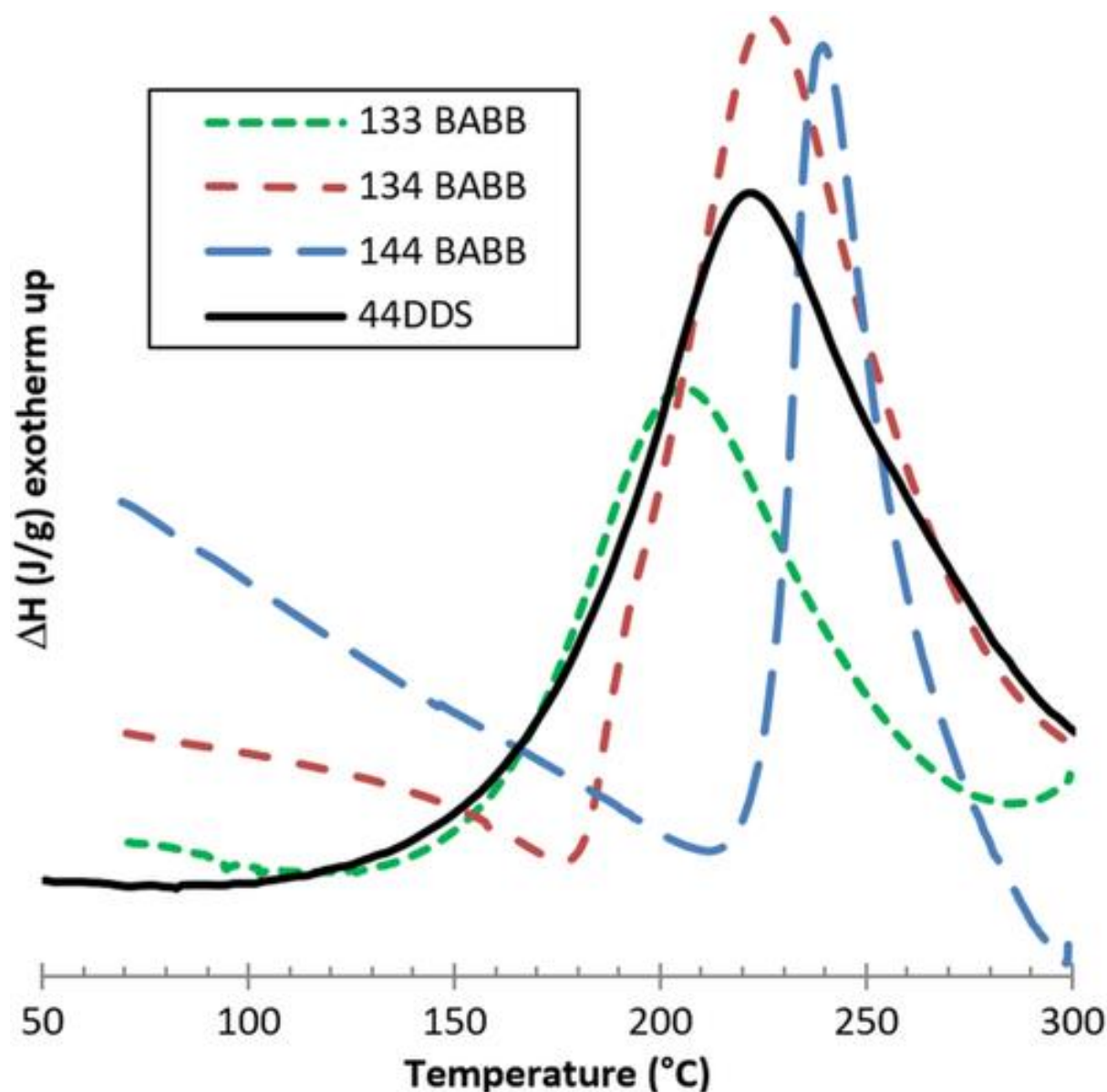


Figure 3

[Open in figure viewerPowerPoint](#)

Dynamic differential scanning calorimetry (DSC) thermograms of the uncured epoxy amine resin systems

Table 1. Summary of the dynamic and isothermal DSC measurements characterizing the rate of cure, reaction kinetics, and glass transition temperatures for the BisA and BisF epoxy amine networks

Epoxy resin	Amine	Dynamic		Isothermal		
		$T_p/T_{onset}(^{\circ}\text{C})$	Peak width 0.5 height	$t_p(\text{min})$	$k_1 (\text{s}^{-1}) (\times 10^{-5})$	$k_2 (\text{s}^{-1}) (\times 10^{-5})$
BisF	133 BABB	204.8/125.7	62	1.45	155.8	299.4
	134 BABB	225.7/176.7	55	10.1	59	229.1
	144 BABB	237.7/212.1	21	63.1	6.2	157
	44 DDS	222.0/97.7	74	6.3	60.5	263.5
BisA	133 BABB	193.4/107	54	1.33	3.7	148.6
	134 BABB	216.0/155	72	9.4	83.9	196.6
	144 BABB	235.7/205	19	51.75	140.6	387.6
	44 DDS	221.0/144	59	5.3	79.2	143.7

- Abbreviations: 133 BABB, 1,3-bis(3-aminobenzoyl)benzene; 134 BABB, 1,3-bis(4-aminobenzoyl)benzene; 144 BABB, 1,4-bis(4-aminobenzoyl)benzene; 44 DDS, 4,4-diaminodiphenyl sulfone; BisA, bisphenol A; BisF, bisphenol F; DSC, differential scanning calorimetry.

To better understand reactivity and reaction kinetics of the resin systems, isothermal curing was performed. Figure 4A shows the isothermal thermograms for the BisF resin systems, which clearly display autocatalytic behavior evident from the rapid increase in heat output

followed immediately by an exponential decline to zero. The time to the maximum rate of cure, t_p , analogous to the T_p discussed previously and also shown in Table 1, displays similar trends to the dynamic DSC studies for both the BisA and BisF epoxy resins. Again, the slowest BABB hardener was 144 BABB, followed by 134 BABB with 133 BABB being the fastest curative. Based upon the t_p , the 44 DDS again displays somewhat intermediate behavior, between the reactivity of the 133 and 134 BABB hardeners for both BisA and BisF epoxy resins. To explore the reaction kinetics, the autocatalytic kinetic model first developed by Horie et al²² was used to calculate rate constants, k_1 and k_2 which represent catalysis from hydroxyl groups present initially and those formed during cure, respectively. The model is shown below:

$$r = (k_1 + k_2\alpha)^m (1-\alpha)^n \quad (1)$$

where k_1 and k_2 are determined by plotting the reduced rate parameter, $r/(1-\alpha)^n$, $r = \frac{d\alpha}{dt}$, as a function of fractional conversion, α . The calculated rate constants are shown in Figure 4B for both epoxy resins, which supports the trends in reactivity already discussed, with 144 BABB being the least reactive, followed by 134 BABB and finally 133 BABB regardless of epoxy resins. Compared with the dynamic DSC studies, the reactivity of the 134 BABB amine is much closer to that of the 133 BABB rather than the 144 BABB, although it remains similar in reactivity to the 44 DDS. To do this modeling, it was assumed that the cure conversion was 100% since DSC analysis of the cured resins displayed no residual exotherm at all, regardless of epoxy resin, amine hardener or whether the initial cure was isothermal or dynamic.

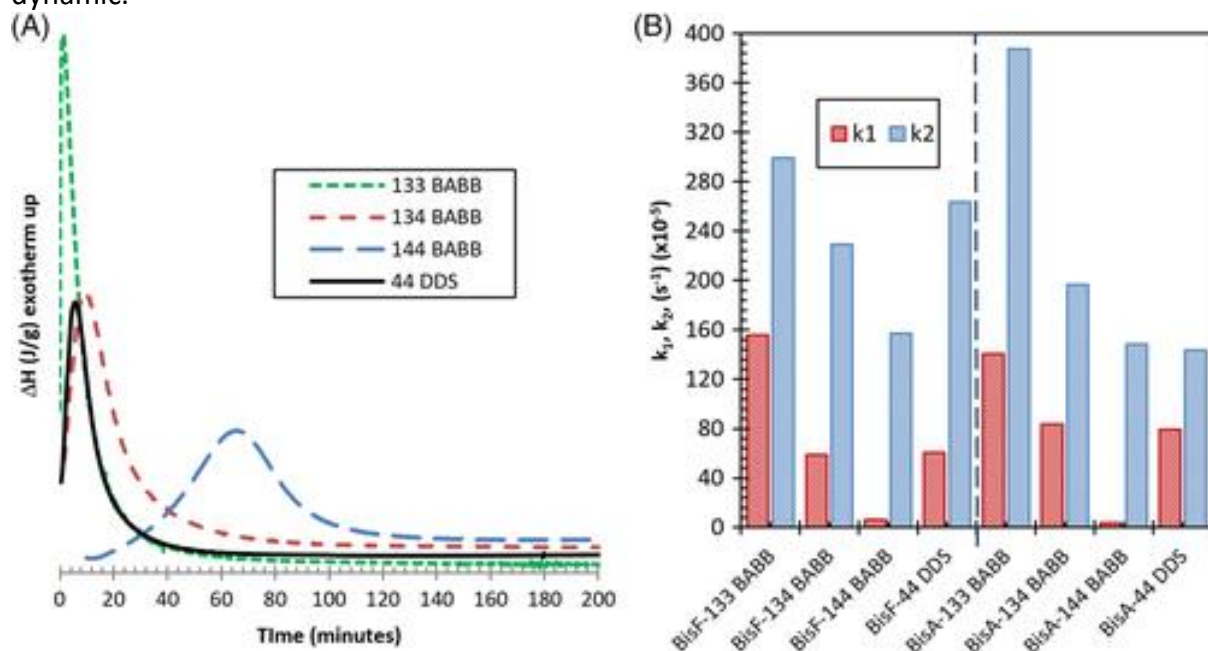


Figure 4

[Open in figure viewer](#) PowerPoint

(A) Isothermal differential scanning calorimetry (DSC) thermograms of the BisF epoxy amine cure at 177°C and (B) a summary of the autocatalytic kinetic rate constants, k_1 and k_2 for each epoxy amine resin system hardener during isothermal cure at 177°C

These results are particularly interesting in light of recent work by Varley et al²⁰ where BisF epoxy resin was cured with similarly substituted isomers of ether linked aromatic amines. The reaction kinetics for tri-aryl ethers displayed higher reactivity due to the ether group being strongly electron donating and added resonance effects preferentially increased reactivity further for para substitution. The reaction kinetics for the BABB systems in this work, however, displayed completely opposite behavior, but for the same reasons. Carbonyl linkages are mildly electron withdrawing instead of donating, so that the inductive electron withdrawing and added resonance effects acted to reduce nucleophilicity and hence reactivity to para substituted amines, comparatively increasing the reactivity of meta substituted amines.

Computational methods calculated the Huckel charge on each amine which broadly predicted the reactivities of the amines, as shown in Table 2. The Huckel charge for 144 BABB was 0.1949 while for 133 BABB it was 0.0998. The higher the Huckel charge, the lower the amine reactivity, so this was in complete accord with experiment. The predicted charge of 0.1889 for the 134 BABB is also consistent in that it displays intermediate behavior between the 144 BABB and 133 BABB, but its similarity to 144 BABB seemed unsatisfactory given experimentally it is much closer to 133 BABB than 144 BABB. The calculated Huckel charge to the 44 DDS was relatively high, but less than the 134 and 144 BABB amines which was somewhat supportive of experimentally obtained kinetics results. To explore this further, Table 2 shows molecular orbital calculations for the C-N bond lengths and amine-to-amine distances which might provide some insight into the variation in reactivity between 134 BABB and 144 BABB. The amine-to-amine distance for 134 BABB (13.216 Å) and 144 BABB (14.610 Å) varies considerably suggesting the spatial configuration of the amines might play a role in controlling reactivity. It is proposed that the more linear and therefore more planar, all para substituted 144 BABB may have greater electron delocalization across the three aromatic rings, thereby enhancing the electron withdrawing ability of the carbonyl and hence further reducing its reactivity.

Table 2. Calculation of structural and electron density parameter for the BABB and 44 DDS amines

	C-N bond lengths (Å)	Amine to amine distance (Å)	Amine charge (e) (Huckel)	Total energy (kcal/mol)
133 BABB	1.267	12.50	0.0909	56.3079

	C-N bond lengths (Å)	Amine to amine distance (Å)	Amine charge (e) (Huckel)	Total energy (kcal/mol)
134 BABB	1.462	13.22	0.1889	27.8875
144 BABB	1.268	14.61	0.1949	55.0446
44 DDS	1.268	9.55	0.1479	181.0745

- Abbreviations: 133 BABB, 1,3-bis(3-aminobenzoyl)benzene; 134 BABB, 1,3-bis(4-aminobenzoyl)benzene; 144 BABB, 1,4-bis(4-aminobenzoyl)benzene; 44 DDS, 4,4-diaminodiphenyl sulfone.

The NIR spectra of the cured networks in Figure 5A,B for the BisF and BisA networks, respectively, qualitatively illustrates the impact of aromatic substitution on the chemical structure of the final network.^{23, 24} In contrast to the DSC results, epoxide consumption does not appear to be 100% as small epoxide peaks appear as shoulders on the much stronger aromatic C-H overtone peaks at about 4580 and 4650 cm⁻¹, respectively. It is difficult to quantify this, but as the aromatic C-H overtone also acts as an internal standard, the extent of conversion is likely to be similar to each other, regardless of BABB substitution. Qualitative differences in the extent of secondary amine conversion, however, is clearly observed in the 6500 and 6800 cm⁻¹ range where increased consumption of the secondary amine peak for the 133 BABB networks is observed as evidenced by the lack of any observable peak at 6700 cm⁻¹. This compares with the 134 BABB, 144 BABB, and 44 DDS cured networks which all display prominent secondary amine peaks and evidence for reduced secondary amine consumption. While not being a direct measure of reaction rate, these results do indeed provide strong support for a more completely cured 133 BABB network regardless of epoxy resin and complements the findings of the DSC studies.

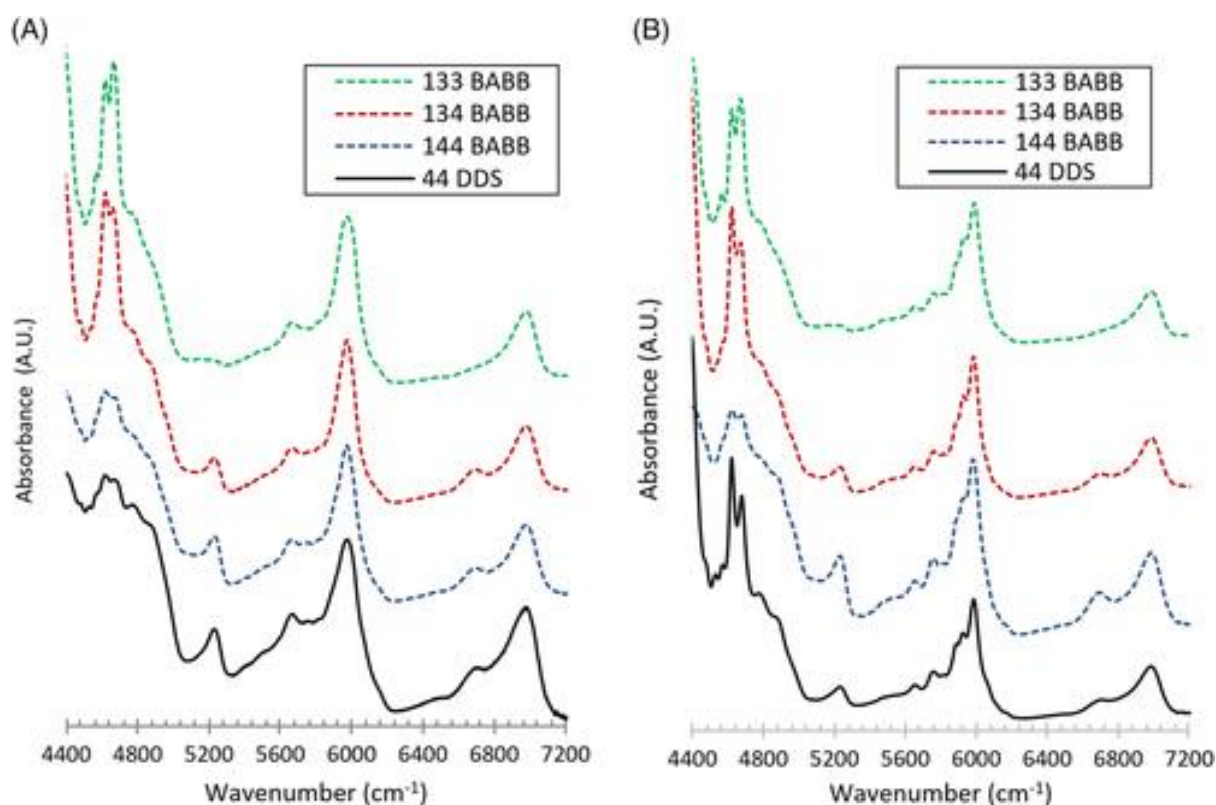


Figure 5

[Open in figure viewer](#) PowerPoint

NIR spectra of the (A) BisF and (B) BisA epoxy amine networks after cure at 177°C for 10 hours

3.2 Thermal properties

The storage modulus and $\tan \delta$ spectra obtained from DMTA and the DSC thermograms are shown in Figure 6A,B, respectively, while the corresponding T_g s are plotted in Figure 6C. DMTA showed that the 133 BABB cured networks consistently had the lowest T_g s at 154.3°C (BisF) and 168.8°C (BisA) ($\tan \delta$ spectra), which increased significantly for 134 BABB (BisF 172.4°C; BisA 188.8°C), followed by a modest decrease for the 144 BABB (BisF 171.9°C; BisA 184.0°C) ($\tan \delta$ spectra) networks. For the DSC measurements in Figure 6B, similar trends were evident, although the lack of a clear endotherm for the 144 BABB networks made it difficult to accurately determine the T_g . Nonetheless, the trends in T_g as a function of aromatic substitution in Figure 6C reveal a significant increase in T_g from 133 BABB to 134 BABB despite a modest reduction for the 144 BABB networks. The T_g for all of the BABB networks were lower than the T_g of the 44 DDS network likely due to the higher crosslink density of 44 DDS and the thermal stability of the sulfone group. The increased T_g for para substituted amines, however, can be attributed to the increased free volume enabling greater short-range molecular motions that dissipate energy but then require further energy to initiate longer range segmental motion.

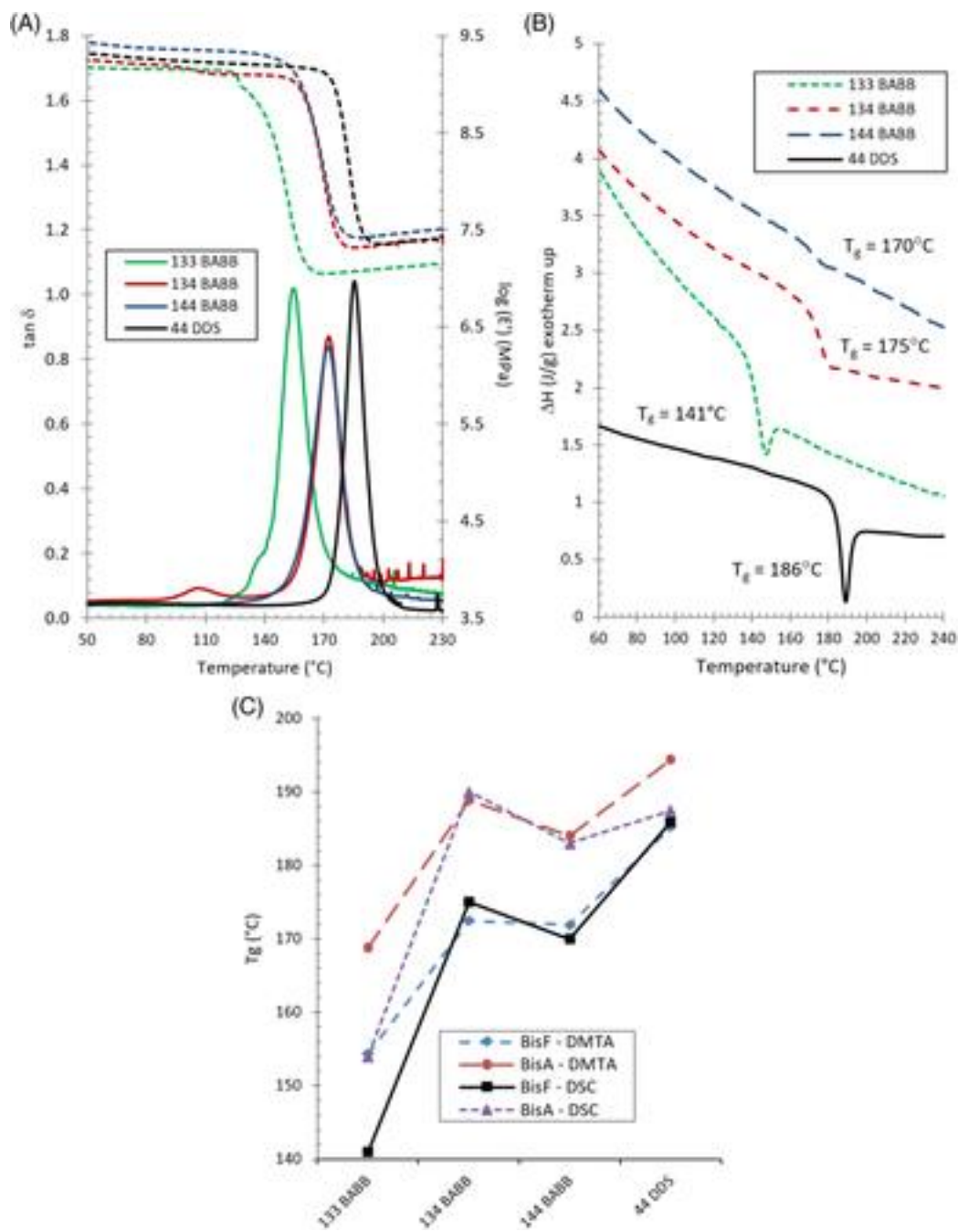


Figure 6
Open in figure viewerPowerPoint

(A) Dynamic mechanical thermal analysis (DMTA) spectra and (B) differential scanning calorimetry (DSC) thermograms of the BisF amine networks after cure at 177°C and (C) a summary plot of all T_g measurements for all of the cured epoxy amine networks

Thermal stability of the cured networks was investigated using TGA shown in Figure 7A for the BisF networks while Figure 7B compares the temperature at 10% weight loss, $T_{10\%}$ and char yields for both the BisA and BisF networks. These results along with the temperature at maximum rate of degradation (T_{max}) are also shown in Table 3. The thermograms in Figure 7A reveal a single degradation step followed by a more stable char region for each system. The 44 DDS networks display the greatest thermal stability as evidenced by

their T_{max} and $T_{10\%}$, although the char yields were significantly lower than the BABB networks. In contrast to previous results, the less thermally stable BABB networks showed no evidence of any trend with aromatic substitution. Reduced thermal stability of the BABB networks compared to the 44 DDS is proposed to be related to the susceptibility to thermal cleavage of the two carbonyl linkages compared with the very stable single sulfone linkage within the 44 DDS.²⁵ The char yields for the BABB networks however, while not showing a clear trend in aromatic substitution were indeed significantly higher compared with the 44 DDS. This is likely due to thermal degradation producing a more stable and highly aromatic char layer compared with the 44 DDS network. This result provides an important indicator for their potential use as inherently fire-retardant polymer networks.

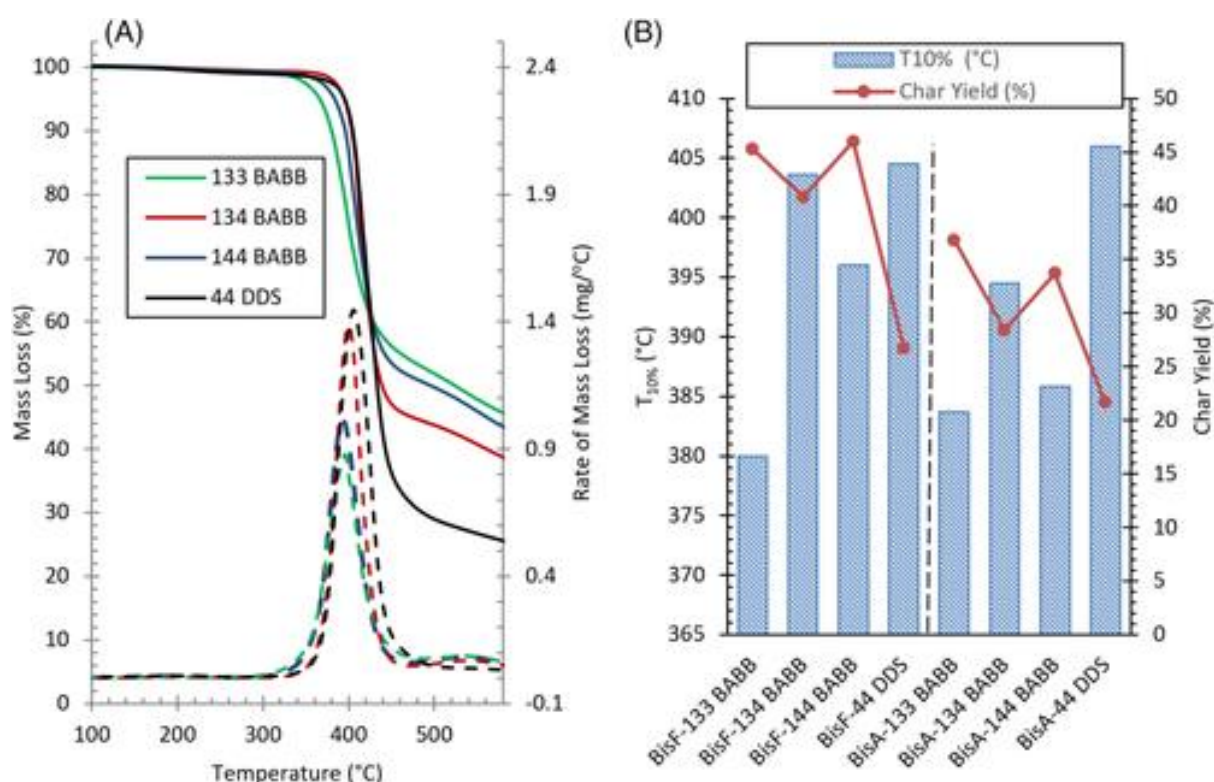


Figure 7

Open in figure viewer PowerPoint

(A) Thermogravimetric analyzer (TGA) thermograms of the BisF epoxy amine networks after cure at 177°C illustrating thermal degradation profile and (B) summary plot of all $T_{10\%}$ and char yield (%) measurements for all of the cured epoxy amine networks

Table 3. Thermal stability measurements using TGA thermal analysis for the BisA and BisF epoxy amine networks

Epoxy resin	Amine	T_{max} (°C)	$T_{10\%}$ (°C)	Char yield (%)
BisF	133 BABB	395.4	380.0	45.3

Epoxy resin	Amine	T_{max} (°C)	$T_{10\%}$ (°C)	Char yield (%)
BisA	134 BABB	399.8	403.6	40.8
	144 BABB	393.2	396.0	46.0
	44 DDS	405.7	404.5	26.7
	133 BABB	397.6	383.7	36.8
	134 BABB	405.8	394.5	28.4
	144 BABB	408.1	385.8	33.7
	44 DDS	417.9	406.0	21.7

- Abbreviations: 133 BABB, 1,3-bis(3-aminobenzoyl)benzene; 134 BABB, 1,3-bis(4-aminobenzoyl)benzene; 144 BABB, 1,4-bis(4-aminobenzoyl)benzene; 44 DDS, 4,4-diaminodiphenyl sulfone; TGA, thermogravimetric analyzer.

3.3 Mechanical properties

The flexural properties of the BisA and BisF networks are shown in Figure 8A-C for the modulus, strength, and displacement at failure, respectively. While there is some scatter in the results, it is clear that the BABB networks have superior properties to the 44 DDS networks with respect to modulus, strength, and displacement to failure. More specifically, the 133 BABB cured network has the highest modulus, followed by the 144 BABB and then 134 BABB, which has a similar value to the 44 DDS shown in Figure 8A. The meta substituted 133 BABB displays the highest modulus due to the combined effect of anti-plasticization, supplementary reinforcement,^{18, 21} and an expected increased equilibrium packing density. As expected, increased para substitution reduced modulus, although the lower 134 BABB compared to 144 BABB was not expected. The ultimate strengths of the BABB networks were again all significantly higher than the 44 DDS networks (BisA-133 BABB 20% higher, BisF-133 BABB 20% higher), but tended to decrease with increasing para substitution, in accord with other studies.^{19, 20, 26} The decreasing strengths reflect reduced supplementary reinforcement and increased phenylene rotations reduce the

required energy to initiate yielding.¹⁹ Figure 8C shows the displacement at failure, used as a measure of toughness or distortional behavior for each of the networks and shows that BABB networks were again higher than 44 DDS, but particularly so for the 134 and 144 BABB networks. This is due to the same short-range phenylene rotations that reduce modulus and strength, now being able to provide an additional energy dissipation mechanism that increases resistance to deformation.^{19, 27}

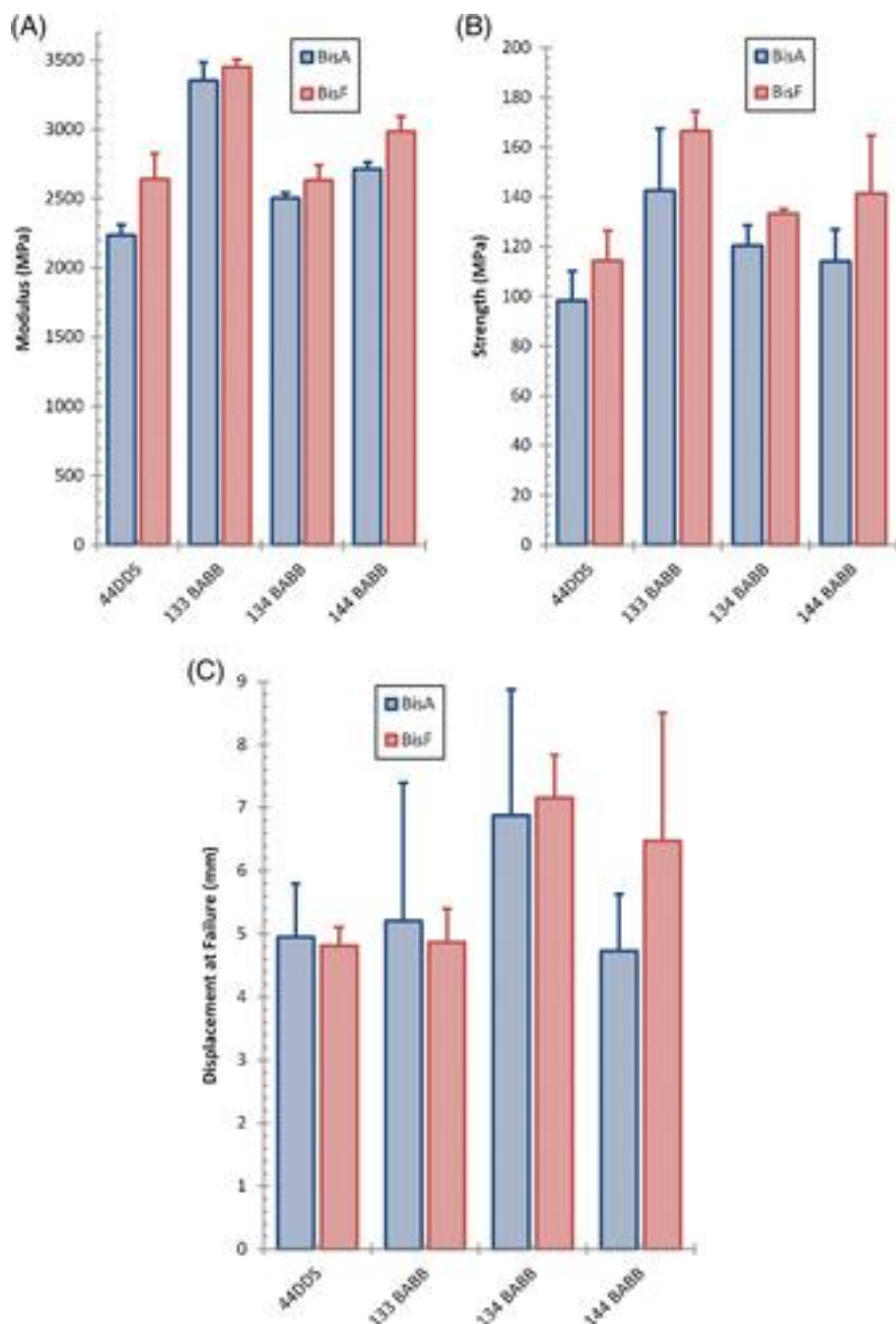


Figure 8

Open in figure viewerPowerPoint

Flexural properties of the epoxy amine networks after cure 177°C including the (A) modulus, (B) strength, and (C) displacement at failure

While all of the BABB networks displayed significantly enhanced mechanical properties compared with 44 DDS, the 134 BABB, however, stood out as having the best balance of properties, in regards to modulus, strength, and toughness. Important to note also, that the previous work by Varley et al,²⁰ showed similar trends with aromatic substitution for the same set of mechanical properties; however, in this study, the modulus and strength were higher, while the displacement to failure significantly lower. It can be proposed therefore that comparatively, the rigidity of the carbonyl linkage restricts both short-range motion and longer segmental motions during deformation, enhancing stiffness and strength, while limiting energy dissipation mechanisms that would otherwise increase displacement to failure or distortional behavior.

4 CONCLUSION

In summary, three tri-aryl ketone amine isomers only varying by their aromatic substitution were synthesized and cured with two commercially available epoxy resins, BisA, and BisF. The electron withdrawing effect of the carbonyl linkages reduced the rate of reaction and inhibited secondary amine conversion as aromatic substitution became increasingly para substituted. Differences in reaction rates between the 134 BABB and 144 BABB hardeners were attributed to spatial configurations impacting the overall conjugation of the aromatic network.

Thermal analysis revealed that the T_g s of the networks increased from 133 BABB to 134 BABB, but a modest reduction in T_g was observed for the 144 BABB network. All of the BABB networks had lower T_g s than the corresponding 44 DDS network. The mechanical properties of the BABB networks, as determined by flexural modulus, strength, and distortional behavior, were significantly superior to the 44 DDS networks, clearly illustrating the value of tri-aryl amines linked by carbonyl groups. Despite a modest reduction in thermal stability compared with the 44 DDS networks, significantly higher char yields were observed.

ACKNOWLEDGEMENTS

Prof R.J.V. also acknowledges funding from the Boeing Company that led to the synthesis of the tri-aryl keto amines. This work was partially supported by The Australian Research Council (DP180100094) and the Office of Naval Research Global (N62909-18-1-2024).